Inorg. Chem. **1992**, *31*, 2079–2085 **2079**

Contribution from the Chemistry Department,
Brookhaven National Laboratory, Upton, New York 11973

Photophysical Properties of Covalently Attached $Ru(bpy)_3{}^{2+}$ and $Mcyclam^{2+}$ ($M = Ni, H_2$) Complexes

Etsuko Fujita,* Steven J. Milder,[1] and Bruce S. Brunschwig

Received September 5, 1991

Absorption and emission spectra, emission quantum yields, and excited-state lifetimes of the metal-to-ligand charge-transfer (MLCT) excited state(s) of $Ru(bpy)_2(6\text{-}Mebpy)^{2+}$, $Ru(bpy)_2(bpy\text{-}cyclamH_2)^{4+}$, and $Ru(bpy)_2(bpy\text{-}cyclamNi)^{4+}$ are reported. The absorption and emission spectra of these complexes are similar to those of $Ru(bpy)_3{}^{2+}$ in H_2O at room temperature except for small shifts in the maxima. The emission lifetime decreases by a factor of about 80 for 6-Mebpy, and the emission quantum yield decreases by a factor of about 300 for the bpy-cyclam pendant complexes as compared to the parent $Ru(bpy)_3{}^{2+}$ complex at 25 °C. Decay of the ^{3}MLCT excited state takes place by two independent channels: a temperature-independent pathway to the ground state and a thermally-activated pathway via a ligand-field excited state. Activation free energies, E_a, for the latter pathway were obtained from fits of the temperature-dependent emission lifetime measurements. Smaller E_a were observed for the 6-substituted complexes (1500–2300 cm^{-1}) relative to $Ru(bpy)_3{}^{2+}$ (3000–3910 cm^{-1}) in EtOH and CH_3CN, indicating that either the energy difference decreases and/or the reorganization parameter changes between the emissive ^{3}MLCT and the ligand-field state to which it is strongly coupled. The smaller E_a can be attributed to the increased Ru–N bond distance in the 6-substituted complexes caused by steric hindrance that decreases the ligand-field strength and lowers the energy and/or reorganization parameter of the ligand-field excited state. For the $bpy\text{-}cyclamNi^{2+}$ pendant complex, an energy-transfer pathway may also provide a deactivation channel.

Introduction

The reduction of CO_2 is the basis for solar energy storage in plants. As a result, there is considerable current interest[2,3] in the synthesis of catalysts that will aid in the reduction of CO_2, though to date, the work has met with only modest success. Schemes employing a separate sensitizer, quencher, and transtion-metal catalyst to active CO_2 have been reported.[4,5] Fisher and Eisenberg[6] have reported the electrochemical activity of various cobalt and nickel tetraazamacrocycle complexes including $NiMe_6cyclam^{2+}$ ($Me_6cyclam$ = 5,7,7,12,14,14-hexamethyl-1,4,8,11-tetraazacyclotetradecane) in the reduction of CO_2 to CO in an acetonitrile/water mixture. Further work by Beley et al.[7] established that $Ni(cyclam)^{2+}$ (cyclam = 1,4,8,11-tetraazacyclotetradecane) shows a remarkably high selectivity for electrochemical reduction of CO_2 relative to the electrochemical reduction of water to H_2. Photochemical reduction of CO_2 has been reported using $Ru(bpy)_3{}^{2+}$ as the sensitizer, $Ni(cyclam)^{2+}$ as the catalyst, and ascorbate as the sacrificial reductive quencher by Grant et al.[5a] This system also produces H_2 via the reduction of water, and the yields of both CO and H_2 are pH dependent. However, the multimolecular systems studied[5] show low yields due to a competing process in the catalytic cycle.

Combining the sensitizer and reduction catalyst into a single molecule[8,9] by covalently attaching a macrocycle to a polypyridyl sensitizer may yield a complex that will be useful in CO_2 reduction. Complexes in which a macrocycle is bound to several polypyridyl–metal complexes have been produced, and their potential multiredox and catalytic features have been studied.[8] $Ru(bpy)_2(bpy\text{-}cyclamM_1)^{4+}$ ($M_1 = H_2$, Ni) complexes have been prepared and characterized by Kimura et al.[9] They reported that the absorption and emission spectra of both pendant complexes are similar to those of $Ru(bpy)_3{}^{2+}$ in H_2O at room temperature, but their room-temperature emission intensities are much lower. They suggested that the lowered emission yields are due to intramolecular quenching. In order to determine if this is the case, the photophysical properties of these complexes, including the temperature dependence of their emission lifetimes, were studied. As a basis for comparison, $Ru(bpy)_2(6\text{-}Mebpy)^{2+}$ was also prepared and studied.[10] A pictorial representation of the pendant complexes, with $M = Ni^{2+}$ or $2H^+$, is shown below.

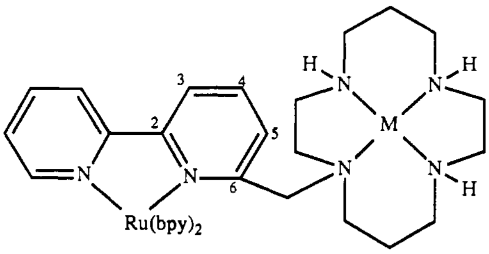

Experimental Section

Materials. The complexes $[Ni(cyclam)](ClO_4)_2$, $[Ni(diene)](ClO_4)_2$ (diene = 5,7,7,12,14,14-hexamethyl-1,4,8,11-tetraazacyclotetradeca-4,11-diene), and $[Ni(tetraene)](ClO_4)_2$ (tetraene = 2,3,9,10-tetramethyl-1,4,8,11-tetraazacyclotetradeca-1,3,8,10-tetraene) were prepared as previously described[11,12] and were characterized by UV–vis, IR, and ^{1}H NMR spectroscopies. (*Warning*: The perchlorate salts used in this study may be explosive and are potentially hazardous.) Analyses for

---

(1) Present address: Division of Natural Sciences, The Evergreen State College, Olympia, WA 98505.

(2) Recent reviews: (a) Creutz, C. In *Electrochemical and Electrocatalytic Reduction of Carbon Dioxide*; Sullivan, B. P., Ed.; Elsevier: Amsterdam; in press. (b) Walther, D. *Coord. Chem. Rev.* **1987**, *79*, 135. (c) Ayers, W. M., Ed. *Catalytic Activation of Carbon Dioxide*; ACS Symposium Series; American Chemical Society: Washington, DC, 1988. (d) Behr, A. *Carbon Dioxide Activation by Metal Complexes*; VCH: Weinheim, 1988. (e) Braunstein, D.; Matt, D.; Nobel, D. *Chem. Rev.* **1988**, *88*, 747. (f) Kolomnikov, I. S.; Lysak, T. V.; Rusakov, S. L.; Kharitonov, Y. Y. *Russ. Chem. Rev.* **1988**, *57*, 406. (g) Behr, A. *Angew. Chem., Int. Ed. Engl.* **1988**, *27*, 661. (h) Collin, J. P.; Sauvage, J. P. *Coord. Chem. Rev.* **1989**, *93*, 245.

(3) See references cited: (a) Fujita, E.; Creutz, C.; Sutin, N.; Szalda, D. J. *J. Am. Chem. Soc.* **1991**, *113*, 343. (b) Fujita, E.; Szalda, D. J.; Creutz, C.; Sutin, N. *J. Am. Chem. Soc.* **1988**, *110*, 4870.

(4) Recent studies of photochemical or photoelectrochemical reduction of CO_2: (a) Ogura, K.; Arima, H. *Chem. Lett.* **1988**, 311. (b) Cook, R. L.; MacDuff, R. C.; Sammells, A. *J. Electrochem. Soc.* **1988**, *135*, 3070. (c) Belmore, K. A.; Vanderpool, R. A.; Tsai, J.-C.; Khan, M. A.; Nicholas, K. M. *J. Am. Chem. Soc.* **1988**, *110*, 2004. (d) Lemke, F. R.; DeLaet, D. L.; Gao, J.; Kubiak, C. P. *J. Am. Chem. Soc.* **1988**, *110*, 6904. (e) Willner, I.; Mandler, D. *J. Am. Chem. Soc.* **1989**, *111*, 1330. (f) Ikeda, S.; Saito, Y.; Yoshida, M.; Noda, H.; Maeda, M.; Ito, K. *J. Electroanal. Chem. Interfacial Electrochem.* **1989**, *260*, 335. (g) Raphael, M. W.; Malati, M. A. *J. Photochem. Photobiol., A* **1989**, *46*, 367. (h) Bockris, J. O'M.; Wass, J. C. *J. Electrochem. Soc.* **1989**, *136*, 2521. (i) Noda, H.; Yamamoto, A.; Ikeda, S.; Maeda, M.; Ito, K. *Chem. Lett.* **1990**, 1757. (j) Inoue, H.; Kubo, Y.; Yoneyama, H. *J. Chem. Soc., Faraday Trans.* **1991**, *87*, 553.

(5) (a) Grant, J. L.; Goswami, K.; Spreer, L. O.; Otvos, J. W.; Calvin, M. *J. Chem. Soc., Dalton Trans.* **1987**, 2105. (b) Craig, C. A.; Spreer, L. O.; Otvos, J. W.; Calvin, M. *J. Phys. Chem.* **1990**, *94*, 7957.

(6) Fisher, B.; Eisenberg, R. *J. Am. Chem. Soc.* **1980**, *102*, 7361.

(7) (a) Beley, M.; Collin, J. P.; Ruppert, R.; Sauvage, J. P. *J. Chem. Soc., Chem. Commun.* **1984**, 1315. (b) Beley, M.; Collin, J. P.; Ruppert, R.; Sauvage, J. P. *J. Am. Chem. Soc.* **1986**, *108*, 7461.

(8) Lehn, J.; Ziessel, R. *J. Chem. Soc., Chem. Commun.* **1987**, 1292.

(9) Kimura, E.; Wada, S.; Shionoya, M.; Takahashi, T.; Iitaka, Y. *J. Chem. Soc., Chem. Commun.* **1990**, 397.

(10) Since the $Co(diene)^{2+}$ (diene = 5,7,7,12,14,14-hexamethyl-1,4,8,11-tetraazacyclotetradeca-4,11-diene) complex was also used as a catalyst for the reduction of CO_2 and H_2O, the preparation of $Ru(bpy)_2(bpy\text{-}dieneM_1)^{4+}$ was attempted, but it was unsuccessful.

(11) (a) Bosnich, B.; Tobe, M. I.; Webb, G. A. *Inorg. Chem.* **1965**, *4*, 1109. (b) Lovecchio, F. V.; Gore, E. S.; Busch, D. H. *J. Am. Chem. Soc.* **1974**, *96*, 3109.

(12) Douglas, B. E., Editor-in-Chief. *Inorganic Syntheses*; Wiley: New York, 1978; Vol. XVIII.

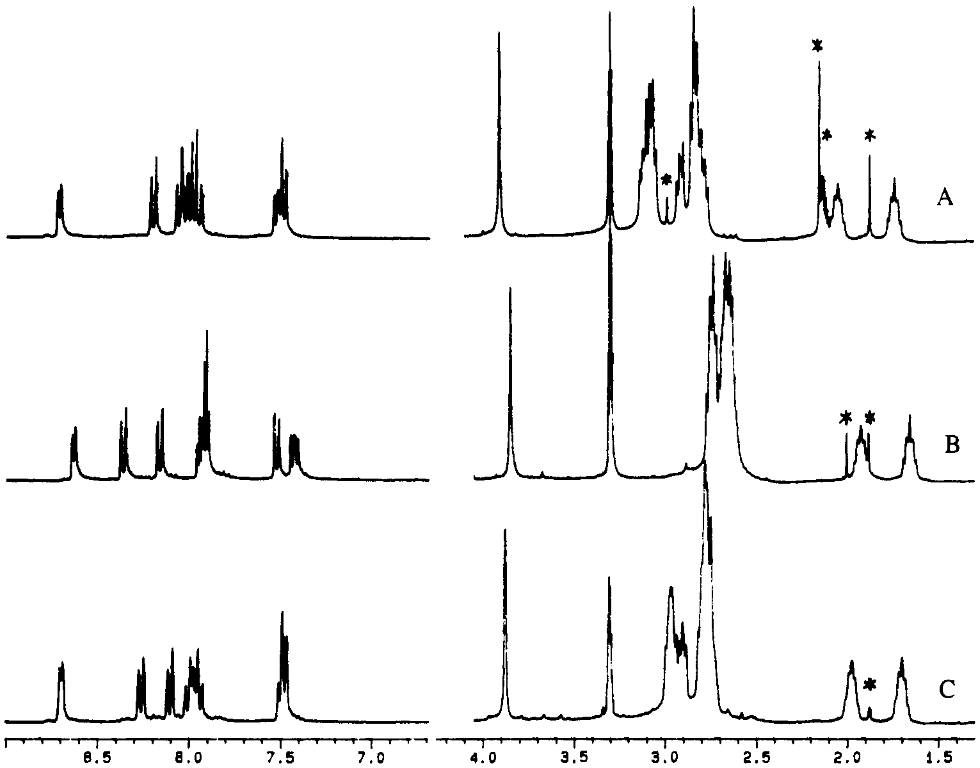

Figure 1. ^1H NMR of the three components, A, B, and C, of bpy-cyclam in CD_3OD. An asterisk indicates impurity peaks. The peaks at 3.3 ppm are due to the solvent.

nickel and anions were satisfactory. All synthesis were carried out using reagent-grade materials. Acetonitrile, ethanol (EtOH), pyridine, and dichloromethane for absorption and emission spectra were purified in the published manner[13] and stored under vacuum over either activated molecular sieves (3A) or CaH_2. Propylene carbonate and *N,N*-dimethylacetamide were used without further purification. The abbreviations of other species to be discussed are bpy = 2,2′-bipyridine, 6-Mebpy = 6-methyl-2,2′-bipyridine, 6-ClMebpy = 6-(chloromethyl)-2,2′-bipyridine, 6-Cl_2Mebpy = 6-(dichloromethyl)-2,2′-bipyridine, 4,4′-Me_2bpy = 4,4′-dimethyl-2,2′-bipyridine, bpy-cyclam = 1-(2,2′-bipyridin-6-ylmethyl)-1,4,8,11-tetraazacyclotetradecane, Me_4cyclam = 1,4,8,11-tetramethyl-1,4,8,11-tetraazacyclotetradecane, HTFMS = trifluoromethanesulfonic acid, and TBACl = tetrabutylammonium chloride.

Preparation of 6-Mebpy, 6-ClMebpy, and bpy-cyclam. The preparation of 6-Mebpy[9] followed the procedures of Kauffmann et al.[14] and Garber et al.[15] The dark oil was distilled at 9.0 Torr to give 6-Mebpy as a yellow oil in 70% yield. ^1H NMR: singlet (3 H) 2.60 ppm, doublet (1 H) 7.08 ppm, split triplet (1 H) 7.20 ppm, triplet (1 H) 7.61 ppm, split triplet (1 H) 7.72 ppm, doublet (1 H) 8.09 ppm, doublet (1 H) 8.32 ppm, doublet (1 H) 8.59 ppm. These are similar to the reported values.[15] MS: *m/e* 170 [M^+, 100]. 6-ClMebpy was prepared by the procedure of Newkome et al.[16] The product mixture contained unreacted 6-Mebpy (11%), 6-ClMebpy (64%), and 6-Cl_2Mebpy (25%) by ^1H NMR. The condensation reaction[17] with cyclam was carried out at room temperature for 48 h without further purification of 6-ClMebpy, since 6-Cl_2Mebpy does not react with cyclam. The reaction mixture was chromatographed on a neutral alumina column to eliminate unreacted starting material. TLC (alumina; Machery-Nagel, Germany) of the bpy-cyclam with MeOH indicated the presence of three components: A (R_f = 0.57), B (R_f = 0.40), and C (R_f = 0.23). Separation by chromatography on a column packed with neutral alumina was difficult due to partial interconversion between components A and C on the column. Component B was ultimately isolated by taking advantage of its high solubility in $CHCl_3$ and ethyl acetate. Component C was the least soluble in $CHCl_3$. Components A, B, and C show similar mass spectra: *m/e* 170 [$Mebpy^+$, 100], 367 [$(M - 1)^+$, 1]. ^1H NMR spectra of the three components in CD_3OD are shown in Figure 1. The three components are assigned either as three isomers of bpy-cyclam that exist due to differences in intramolecular hydrogen bonding between the bpy–N and the cyclam–NH or as three species of bpy-cyclam with different levels of protonation. The nature of the differences between the components was not studied further. Component C, which could be separated easily, was used in the experiments discussed below.

Preparation of $Ru(bpy)_2(bpy\text{-}cyclamH_2)(PF_6)_4 \cdot 3H_2O$. A 100-mL EtOH/water solution (v/v = 2) containing 203 mg (0.57 mM) of bpy-cyclam and 297 mg (0.57 mM) of $Ru(bpy)_2Cl_2 \cdot 2H_2O$ was refluxed for 2 h under Ar. The resulting reaction mixture was evaporated to dryness, 30 mL of H_2O was added to the residue, and the unreacted $Ru(bpy)_2Cl_2$ was removed by filtration. The pH of the resultant aqueous solution was adjusted to ca. 2.8 by the addition of HTFMS, and an orange powder was obtained upon addition of NH_4PF_6, which was collected and washed with H_2O. The yield of this crude product was 84%. The PF_6^- salt was dissolved in acetone, and the complex was obtained as the solid Cl^- salt upon addition of TBACl to the solution. The Cl^- salt was purified with the aid of a Sephadex C-25 cation-exchange column with aqueous (0.0–0.4 M) KTFMS as the eluent. Pure $Ru(bpy)_2(bpy\text{-}cyclamH_2)(PF_6)_4 \cdot 3H_2O$ was obtained upon the addition of NH_4PF_6 to the 0.4 M KTFMS solution. Anal.: Ru obs 7.01, calc 7.13; PF_6^- obs 39.6, calc 40.9. ^{13}C NMR in CD_3CN: 22.86, 25.38, 45.36, 46.09, 47.04, 47.45, 50.47, 51.33, 52.33 (2), 61.52, 124.06, 125.50, 125.70 (2), 125.79 (2), 126.15, 128.39, 128.81, 128.85, 128.95, 129.05, 139.04, 139.18 (3), 139.35, 140.41, 152.32, 152.48, 152.70, 153.21, 154.22, 157.87, 158.08, 158.13, 158.16, 158.92, 159.34, 164.90 ppm (reference $SiMe_4$ at 0 ppm; number of carbon atoms in parentheses). UV–vis in H_2O, λ_{max} ($\epsilon \times 10^{-3}$): 448 (12.1), 420 sh (10.0), 350 sh (5.40), 286 (72.0), 254 sh (20.4), 244 (22.7). Titration of $Ru(bpy)_2(bpy\text{-}cyclamH_2)(PF_6)_4$ with NaOH gives pK_a values of 5.5 ± 0.3 and 8.5 ± 0.3.

Preparation of $Ru(bpy)_2(bpy\text{-}cyclamNi)(PF_6)_4 \cdot 3H_2O$. A 50-mL MeOH solution containing 100 mg (0.071 mM) of $Ru(bpy)_2(bpy\text{-}cyclamH_2)(PF_6)_4 \cdot 3H_2O$ and 250 mg (1 mM) of nickel acetate was refluxed for 2 h under Ar. The solvent was removed by rotary evaporation, and the residue was dissolved in H_2O; $Ru(bpy)_2(bpy\text{-}cyclamNi)(PF_6)_4$ was obtained upon addition of NH_4PF_6, and the filtered product was washed with H_2O. The yield of the product was 55%. Anal.: Ru obs 7.0, calc 6.85; Ni obs 3.7, calc 3.98; PF_6^- obs 39.5, calc 39.3. ^{13}C NMR: cyclam signals of major isomer at 23.44, 26.44, 48.41, 48.60, 48.85, 49.88, 50.51, 52.14, 57.82, 58.95, 63.40 (bridging CH_2) ppm; cyclam signals of minor isomer at 22.74, 26.44, 48.41, 48.60, 48.85, 49.88, 50.92, 52.14, 57.46, 58.66, 62.83 (bridging CH_2) ppm. Signals due to bpy ligands were not

---

(13) Riddick, J. A.; Bunger, W. B.; Sakano, T. K. *Organic Solvents, Physical Properties and Methods of Purification*, 4th ed.; Wiley: New York, 1986.

(14) Kauffmann, T.; Konig, J.; Wolterman, A. *Chem. Ber.* **1976**, *109*, 3864.

(15) Garber, T.; Wallendael, S. V.; Rillema, D. P.; Kirk, M.; Hatfield, W. E.; Welch, J. H.; Singh, P. *Inorg. Chem.* **1990**, *29*, 2863.

(16) Newkome, G. R.; Puckett, W. E.; Kiefer, G. E.; Gupta, V. K.; Xia, Y.; Coreil, M.; Hackney, M. *J. Org. Chem.* **1982**, *47*, 4166.

(17) Alcock, N. W.; McLaren, F.; Moore, P.; Pike, G. A.; Roe, S. M. *J. Chem. Soc., Chem. Commun.* **1989**, 629.

well resolved. No signals were observed from the residual metal-free cyclam pendant complex in ^{13}C and ^1H NMR. UV-vis in H_2O, λ_{max} ($\epsilon \times 10^{-3}$): 446 (13.4), 420 sh (10.7), 350 sh (6.15), 286 (79.5), 254 sh (27.1), 244 (30.7).

Preparation of $Ru(bpy)_2(6\text{-}Mebpy)(PF_6)_2$. An 80-mL EtOH/water solution (v/v = 2) containing 200 mg (1.18 mM) of 6-Mebpy and 450 mg (0.87 mM) of $Ru(bpy)_2Cl_2{\cdot}2H_2O$ was refluxed for 30 min under Ar. The resulting reaction mixture was evaporated to dryness. The residue was dissolved in 25 mL of H_2O, and unreacted $Ru(bpy)_2Cl_2$ was removed by filtration. Upon addition of NH_4PF_6 an orange powder was produced, which was collected and washed with H_2O. The yield of the crude product was 96%. A 5% impurity of $Ru(bpy)_3(PF_6)_2$, determined by the integration of the ^1H NMR signals, could not be removed by either repeated recrystallization from acetone/MeOH mixtures or Sephadex LH-20 column chromatography with MeOH. ^{13}C NMR: 26.46, 122.91, 125.28, 125.42, 125.47, 125.54, 125.69, 128.06, 128.46 (2), 128.67, 128.91, 129.52, 138.52, 138.67, 138.80 (2), 139.07, 139.24, 152.19, 152.33, 152.42, 152.69, 154.11, 157.71, 158.07, 158.20, 158.31, 158.35, 159.32, 166.31. UV-vis in H_2O, λ_{max} ($\epsilon \times 10^{-3}$): 450 (14.3), 430 sh (12.4), 350 sh (6.30), 286 (84.2), 254 sh (23.1), 244 (25.7).

Spectroscopic Measurements. Deoxygenated solutions for UV-vis and emission measurements were prepared by repeated freeze-pump-thaw cycles for the solvents H_2O, propylene carbonate, and *N,N*-dimethylacetamide or by vacuum distillation of purified and degassed solvents for the others. The reduced species [(1-3) × 10^{-5} M solutions] were made under vacuum by sodium amalgam (Na-Hg, 0.5% Na in Hg) reduction in sealed glassware equipped with an optical cell. UV-vis spectra were measured on a Hewlett-Packard 8452 diode array spectrophotometer or a Cary 210 spectrometer.

Emission spectra were measured on a home-built apparatus. Excitation was with a 150-W Xe lamp whose output was wavelength selected with a 0.22-m monochromator and chopped. The emission was dispersed by a 0.5-m monochromator with a 600 groove/mm grating blazed at 500 nm and detected by a Hamamatsu R1464 photomultiplier. Standard phase-sensitive electronics were used. The spectra were corrected for the wavelength response of the instrument by comparison with a standardized lamp. Quantum yields, Φ_r, were obtained by measuring the area under the corrected spectrum. $Ru(bpy)_3^{2+}$ was used as the standard, and a value of the emission quantum yield of 0.042 at 25 °C in H_2O was used.[18] Solvent corrections to Φ_r were made with $\Phi_r = \Phi_r^{obs}n^2/n^2_{H_2O}$, where n and n_{H_2O} are the refractive indices of the solvent and water, respectively.[19,20]

Emission lifetimes were determined after excitation of the samples with the third harmonic of a Nd:YAG laser that had been actively/passively mode locked and amplified three times. Either a streak/CCD camera or a fast digitizer detection system was used, depending on whether the lifetime was shorter or longer than 5 ns. For the shorter lifetimes, the sample was excited by a vertically polarized 355-nm 25-35-ps laser pulse, and the emission was collected from the front face of the sample through a polarizer set at 54.7° from vertical, to avoid photoselection artifacts in the observed temporal decay. The collected emission was focused onto a 0.25-mm slit of a 0.22-m polychromator with a 150 groove/mm grating and was dispersed across the horizontal entrance slit of a streak/CCD camera detection system (Hamamatsu M1952 high-speed streak unit, C3140 camera head, C2280 temporal analyzer). This afforded data with both temporal and spectral information. The streak/CCD camera results were corrected for nonlinearities in their sensitivity, but the data were not corrected for the wavelength response of the photocathode or monochromator. Collected simultaneously with the emission was a small portion of the exciting laser light, so as to provide information on the instrument response time, which was typically 35-40 ps. For the longer lifetimes, the emission was focused into a 0.1-m double monochromator and detected by a Hamamatsu R928 photomultiplier whose output was amplified by a home-built amplifier and then digitized by either a LeCroy TR8828D transient digitizer whose fastest digitization rate is 5 ns/point or a HP54510A digital oscilloscope whose fastest digitization rate is 1 ns/point. The kinetics of the signal-averaged data obtained with either detection system were analyzed with standard nonlinear least-squares routines.

Transient absorption spectra were obtained with an intensified diode array system with a 10-ns gate. After passage through the sample, the probe beam from a pulsed Xe lamp was focused into a 0.25-m polychromator whose output was detected by a Princeton Instruments intensified linear diode array. Data were signal averaged and corrected for dark current. Changes in absorption spectra were obtained at specified times after laser excitation of the sample by taking the log of the ratio of the signal without and with laser excitation of the sample.

For the temperature-dependent emission-lifetime studies, the sample was placed in the head of a CVI Cryogenics cryostat controlled by a Lake Shore Cryotronics DCR 80C controller. Typically, the temperature could be maintained to within a range of ±2 °C, and between 100 and 2000 averages were taken for each determination of the emission lifetime at each temperature. For each complex studied, the observed lifetimes could be reproduced to within 2% at a given temperature. For $Ru(bpy)_3^{2+}$ and $Ru(bpy)_2(6\text{-}Mebpy)^{2+}$ the emission lifetimes were measured between 230 and 298 K in CH_3CN and between 165 and 298 K in EtOH, while for $Ru(bpy)_2(bpy\text{-}cyclamH_2)^{4+}$ they were measured between 230 and 272 K in CH_3CN and between 165 and 265 K in EtOH, and for $Ru(bpy)_2(bpy\text{-}cyclamNi)^{4+}$ they were measured between 230 and 266 K in CH_3CN and between 165 and 235 K in EtOH.

Determination of the bimolecular-quenching rate of $Ru(bpy)_3^{2+}$ (5.5 × 10^{-2} M) by the Ni^{II} macrocycles was carried out in 0.5 M KTFMS at 20 °C. For the quenching with $H_2cyclam^{2+}$ 0.5 M HTFMS was used. Quencher concentrations were between 0 and 12 mM. Quenching rate constants, k_q, were calculated from the decrease in the excited-state lifetime as a function of quencher concentration.

The IR spectra were measured on a Mattson Polaris FT-IR spectrometer. ^1H and ^{13}C NMR spectra were obtained on a Bruker AM-300 spectrometer. Mass spectra were measured on a Finnigan MAT 5100 GC/MS system.

Electrochemical Measurements. Cyclic voltammograms were obtained on a BAS100 instrument with scan rates ranging from 10 mV s^{-1} to 1 V s^{-1}. Solutions contained 1 mM ruthenium complex and 0.1 M tetrapropylammonium perchlorate in CH_3CN. A conventional H-type cell was used. Graphite, Pt, and SCE were used as working, counter, and reference electrodes, respectively. Ferrocene was used as an internal standard.

Results

Spectroscopic Properties. The ^{13}C NMR spectrum of $Ru(bpy)_2(bpy\text{-}cyclamNi)(PF_6)_4$ in CD_3CN, in which nickel is low spin and is in a square-planar geometry, suggests the presence of two isomers. A total of 16 signals were observed for the 10 cyclam carbon atoms and the single bridging methylene carbon atom. Six of the peaks were observed as singlets while 10 of the peaks were observed as five doublets. The doublets all have peak ratios of ~2:1 with the intensities of the larger doublet peaks less than the intensities of the six unsplit singlets. This splitting of some of the resonances suggests the presence of two conformers in the sample. The ^1H NMR of this complex shows two signals at very low field: a broad signal at 11.83 ppm and a doublet at 11.68 ppm (J = 7.32 Hz). The total integrated intensity of the two signals equals the intensity expected for a single proton, and the intensity ratio of these two signals is ~1.5. These signals have previously been assigned[9] to a bipyridine proton (5-H) that is in close proximity to the nickel for the two isomers shown below. The chemical shifts of the cyclam protons also indicate the existence of two isomers. On the other hand, the ^1H and ^{13}C NMR of $Ru(bpy)_2(bpy\text{-}cyclamH_2)^{4+}$ show a single species, which is probably due to either fast exchange between the conformers or the predominance of one of the conformers at room temperature in solution. The two isomers of the $Ru(bpy)_2(bpy\text{-}cyclamNi)^{4+}$ could not be separated and were used together.

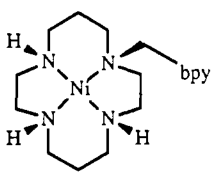

R,S,R,S isomer

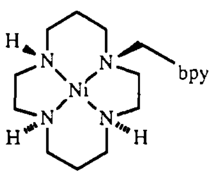

R,R,S,S isomer

The electrochemical properties, absorption and emission spectra, and emission quantum yields at 25 °C and the representative lifetimes of these Ru complexes at various temperatures are summarized in Table I. The temperature dependence of the lifetime of the emission of $Ru(bpy)_3^{2+}$, $Ru(bpy)_2(6\text{-}Mebpy)^{2+}$, $Ru(bpy)_2(bpy\text{-}cyclamH_2)^{4+}$, and $Ru(bpy)_2(bpy\text{-}cyclamNi)^{4+}$ was measured in EtOH and CH_3CN. Shown in Figure 2 is a plot of the log of the observed radiative rate constant ($1/\tau$) versus the

---

(18) (a) Van Houten, J.; Watts, R. J. *J. Am. Chem. Soc.* **1975**, *97*, 3843. (b) Van Houten, J.; Watts, R. J. *J. Am. Chem. Soc.* **1976**, *98*, 4853.

(19) Demas, J. N.; Crosby, G. A. *J. Phys. Chem.* **1971**, *75*, 991.

(20) (a) Caspar, J. V.; Meyer, T. J. *J. Am. Chem. Soc.* **1983**, *105*, 5583. (b) Barigelletti, F.; Juris, A.; Balzani, V.; Belser, P.; von Zelewsky, A. *J. Phys. Chem.* **1987**, *91*, 1095.

Table I. Physical Properties of $Ru(bpy)_2L^{n+}$ Complexes

L	solvent	bpy	6-Mebpy[a]	bpy-cyclamH_2	bpy-cyclamNi
$E_{1/2}$ vs SCE	CH_3CN	1.27	1.27	1.34	1.38
					−1.00
		−1.34	−1.34	−1.33	−1.32
		−1.53	−1.52	−1.53	−1.53
		−1.77	−1.74	−1.79	−1.76
UV–vis					
λ_{max} ($\epsilon \times 10^{-3}$)	H_2O	452 (14.4)	450 (14.3)	448 (12.1)	446 (13.4)
	CH_3CN	451	449	448	446
	EtOH	451	449	448	446
emission					
λ_{max} at 298 K	H_2O	624		626	635
	CH_3CN	620[b]		621	637
	EtOH	612		616	645
λ_{max} at 77 K	EtOH	580, 631	582, 632	592, 632	582, 628
MLCT lifetime					
at 298 K, ns	EtOH	670	8	2	
at 165 K, ns	EtOH	1920	1600	1200, 170[c]	850, 54[c]
Ru–N distance		av 2.056 (6)[d]			av 2.072 (6)[e]

[a] The complex contains 5% $Ru(bpy)_3^{2+}$ as an impurity. [b] From ref 20. [c] Emission data fit to a biexponential decay function. [d] From ref 32. [e] From ref 9, one Ru–N is as long as 2.143 Å.

Table II. Solvent Dependence of the Emission from the $Ru(bpy)_2(bpy\text{-}cyclamH_2)^{4+}$ and the $Ru(bpy)_2(bpy\text{-}cyclamNi)^{4+}$ MLCT Excited States at 25 °C[a]

	$Ru(bpy)_2(bpy\text{-}cyclamH_2)^{4+}$				$Ru(bpy)_2(bpy\text{-}cyclamNi)^{4+}$		
solvent	λ_{max}, nm	ν_{max}, $cm^{-1} \times 10^3$	$\Phi_r \times 10^4$	τ (ns)	λ_{max}, nm	ν_{max}, $cm^{-1} \times 10^3$	$\Phi_r \times 10^4$
CH_2Cl_2	610	16.39	0.63	1			
EtOH	616	16.23	1.4	2	645	15.50	1.1
CH_3CN	621	16.10	1.3	2	637	15.69	2.0
pyridine[b]	627	15.94	4.6	2	642	15.58	5.1
H_2O	626	15.97	3.3	4	635	15.75	1.1
propylene carbonate	622	16.08	3.0	4	645	15.55	1.7
dimethylacetamide	635	15.74	5.7	4	632	15.87	2.4

[a] Φ_r is corrected with $\Phi_r = \Phi_r^{obs}n^2/n^2_{H_2O}$, where n and n_{H_2O} are the refractive indices of the solvent and water, respectively. [b] In pyridine, $Ru(bpy)_2(bpy\text{-}cyclamH_2)^{4+}$ is deprotonated.

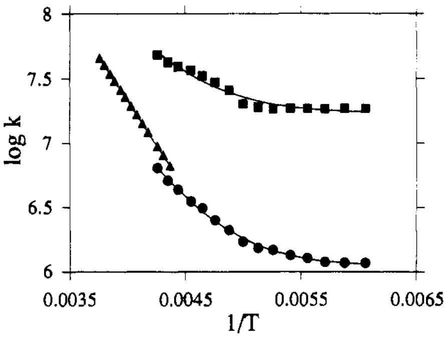

Figure 2. Plot of the logarithm of the observed rate of decay of the ^{3}MLCT emission from $Ru(bpy)_2(bpy\text{-}cyclamNi)^{4+}$ versus the reciprocal of the temperature for (▲) CH_3CN, (●) the slow component in EtOH, and (■) the fast component in EtOH. Lines represent the best nonlinear least-squares fits to the data by eqs 1 and 2.

Table III. Bimolecular Quenching of $Ru(bpy)_3^{2+}$ in Aqueous Solution at 20 °C

quencher	λ_{max} (ϵ),[a] nm (M^{-1} cm^{-1})	$E_{1/2}$,[a] V vs NHE	k_q[b] $\times 10^{-8}$, M^{-1} s^{-1}	k_e[c] $\times 10^{-8}$, s^{-1}
$H_2cyclam^{2+}$			<0.15[d]	
$Ni(cyclam)^{2+}$	445 (42)	−1.21, 1.26	1.5	3
$Ni(diene)^{2+}$	438 (90)	−0.98, 1.57	1.1	2
$Ni(tetraene)^{2+}$	415 sh (2240)	−0.26	22	44

[a] Measured in CH_3CN. [b] Measured in 0.5 M KTFMS solution (with nickel complexes) or 0.5 M HTFMS solution (with cyclam). Quenching rate constants, k_q, were calculated from the decrease in the excited-state lifetime as a function of the concentration of the quencher. [c] k_e is the estimated unimolecular rate constant from $k_q = K_{eq}k_e$; see text for details. [d] Stern–Volmer plot of emission intensities yields $k_q = 0.063 \times 10^8$ M^{-1} s^{-1} at 25 °C.

reciprocal of the temperature for the bpy-cyclamNi^{2+} pendant complex. Table II presents the visible absorption and emission maxima, the emission quantum yields of the two pendant complexes, and the emission lifetime of the nonmetalated pendant complex in various solvents at 25 °C.[21] As previously reported,[9] the absorption and emission spectra of these complexes are similar to those of $Ru(bpy)_3^{2+}$ in H_2O at room temperature, there being only small shifts in the maxima (see Table I). In $Ru(bpy)_2L^{n+}$ (n = 2, 4), the MLCT band shows a blue shift that increases for L in the order bpy, 6-Mebpy, bpy-cyclamH_2^{2+}, and bpy-cyclamNi^{2+}, while the emission maximum of $Ru(bpy)_2(bpy\text{-}cyclamNi)^{4+}$ is somewhat red-shifted relative to the other complexes. At room temperature in EtOH the emission lifetime decreases by a factor of 80 for 6-Mebpy, and the emission quantum yield decreases by a factor of 300 for the cyclam pendant complexes as compared to the parent $Ru(bpy)_3^{2+}$ complex. The emission lifetimes of all of the complexes increase with decreasing temperature. In EtOH the time dependence of the emission of both pendant complexes could not be fit by a single exponential, but biexponential fits were adequate. For the bpy-cyclamH_2^{2+} pendant complex in EtOH, the fast component accounts for 40% of the amplitude of the decay at 165 K and 75% of the amplitude at 265 K. For the bpy-cyclamNi^{2+} pendant complex in EtOH, the fast component of the decay is about 75% of the amplitude at all the temperatures at which it was studied. The biexponential decay

---

(21) Analysis of the emission decay of the bpy-cyclamNi^{2+} pendant complex in EtOH at 25 °C was difficult due to the lifetimes of the species and limitations of the detection equipment. Using the transient digitizer detection system, two decays are observed. One is faster than the bandwidth of the digitizer. The slow decay rate is ~10^7 s^{-1}; however, this rate could not be accurately determined because of the presence of the faster component. Using the streak/CCD camera system, two decays were observed with decay rates of 10^9 and 10^8 s^{-1}. Since the streak/CCD data are limited to times shorter than 4 ns, the slowest decay observed with the transient digitizer system could not be seen with this detection system. Moreover, the intermediate decay is only partially observed. As a consequence, accurate decay rates could not be obtained from the streak/CCD data, and only estimates could be made. The two slower decays correlate with the extrapolation to 25 °C of the lifetimes for the two processes seen at lower temperatures.

Table IV. Parameters Obtained from the Fit of the Temperature Dependence of the Emission Lifetime of $Ru(bpy)_2L^{n+}$ with Equations 1 and 2

L	solvent		k_0, s^{-1}	A, s^{-1} $cm^{1/2}$	E_a, cm^{-1}	$A(kT)^{-1/2}$, s^{-1} $T = 298$ K	k_1, s^{-1} [b] $T = 298$ K
bpy	CH_3CN		5.4×10^5	1.3×10^{15}	3910	9.0×10^{13}	6.2×10^5
bpy	EtOH		5.4×10^5	2.0×10^{13}	3000	1.4×10^{12}	7.6×10^5
6-Mebpy	CH_3CN		$<2.0 \times 10^6$	1.6×10^{13}	2120	1.1×10^{12}	4.1×10^7
6-Mebpy	EtOH		5.8×10^5	6.1×10^{13}	2240	4.2×10^{12}	8.8×10^7
bpy-cyclamH_2	CH_3CN		$<8.0 \times 10^6$	5.1×10^{13}	2110	3.5×10^{12}	1.4×10^8
bpy-cyclamH_2	EtOH	slow[a]	7.9×10^5	4.8×10^{11}	1560	3.3×10^{10}	1.8×10^7
		fast[a]	6.2×10^6	2.8×10^{12}	1590	1.9×10^{11}	9.1×10^7
bpy-cyclamNi	CH_3CN		$<6.0 \times 10^6$	1.4×10^{14}	2280	9.7×10^{12}	1.7×10^8
bpy-cyclamNi	EtOH	slow[a]	1.1×10^6	1.3×10^{13}	1980	9.0×10^{11}	6.6×10^7
		fast[a]	1.7×10^7	1.9×10^{13}	1750	1.3×10^{12}	2.9×10^8

[a] Slow and fast components obtained from fit of emission data by a biexponential decay function. [b] Calculated from eq 2 and values of A and E_a.

of the excited-state emission suggests that the isomers (shown above) of the pendant complexes have different lifetimes. For $Ru(bpy)_2(6\text{-}Mebpy)^{2+}$, the decay of the excited-state emission was also observed to be biexponential; however, the slower, smaller component could be attributed to the presence of ~5% $Ru(bpy)_3^{2+}$ as an impurity in our sample.

Electrochemical Properties. Electrochemical data for all the complexes studied are shown in Table I; this table also contains data for $Ru(bpy)_3^{2+}$. Cyclic voltammograms (CV) for $Ru(bpy)_2(bpy\text{-}cyclamNi)^{4+}$ show a reduction wave due to the $Ni^{II/I}$ at −1.00 V vs SCE. The CV becomes slightly irreversible for scan rates of less than 100 mV s^{-1}.

Bimolecular Quenching. In order to investigate whether electron and/or energy transfer might occur from the emissive ^3MLCT state to Ni^{2+} in the pendant complex, the bimolecular quenching of $Ru(bpy)_3^{2+}$ by several nickel complexes of the ligands was studied. The observed quenching rate constants are shown in Table III.

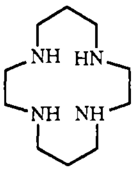
cyclam

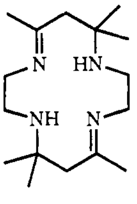
diene

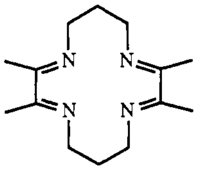
tetraene

Discussion

The $Ni^{II/I}$ reduction potential for $Ru(bpy)_2(bpy\text{-}cyclamNi)^{4+}$, −1.00 V vs SCE, is 0.45 V more positive than the value reported for $Ni(cyclam)^{2+}$ ($E_{1/2} = -1.45$ V)[6,22] but more negative than that observed for $NiMe_4cyclam^{2+}$ (Me_4cyclam = 1,4,8,11-tetramethyl-1,4,8,11-tetraazacyclotetradecane; $E_{1/2} = -0.82$ V).[23] This shift is in the direction expected for an N-alkyl group and may also reflect the interaction between the bpy proton and the nickel center observed both in the ^1H NMR spectrum and in the X-ray structure.[9] The three reduction potentials of the bpy ligands are the same in all four complexes studied. In accord with this observation, the optical spectra of the mono-, di-, and trireduced $Ru(bpy)_2(bpy\text{-}cyclamH_2)^{4+}$ are almost identical to the spectra obtained upon the reduction of $Ru(bpy)_3^{2+}$,[24] indicating that the bpy orbitals are not significantly perturbed by the substitution. In the case of $Ru(bpy)_2(bpy\text{-}cyclamNi)^{4+}$, the first bpy reduction was irreversible and resulted in the elimination of nickel from the cyclam; the spectra after further reduction are the same as those observed in the reductions of $Ru(bpy)_2(bpy\text{-}cyclamH_2)^{4+}$ and $Ru(bpy)_3^{2+}$. The $Ru^{III/II}$ potentials become more positive for L in the series bpy, 6-Mebpy, bpy-cyclamH_2^{2+}, and bpy-cyclamNi^{2+}, with the largest change occurring between the 6-Mebpy and the bpy-cyclamH_2^{2+} complexes. The total shift of 0.11 V is in the opposite direction expected from the electron-donating properties of the methyl or methylene groups in these complexes. For example, the $Ru^{III/II}$ potentials for $Ru(bpy)_n(4,4'\text{-}Me_2bpy)_{3-n}^{2+}$ (n = 0, 1, 2, and 3) in acetonitrile[25,26] are 1.28, 1.24, 1.21, and 1.12 (V vs SCE), respectively, a shift of −0.16 V. Therefore, the shifts of the potentials in the pendant complexes are dominated by other factors, such as geometry changes that occur around the Ru (vide infra).

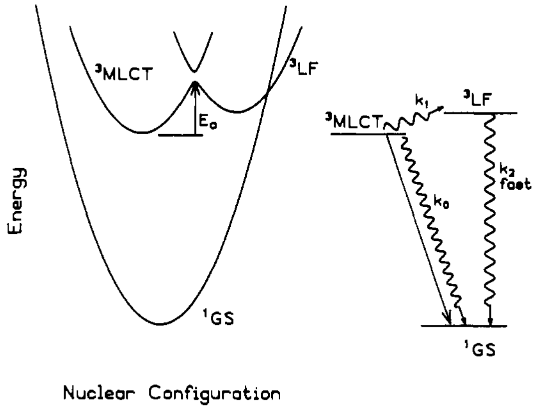

Figure 3. Energy state diagram for $Ru(bpy)_2L^{n+}$ (L = bpy, 6-Mebpy, bpy-cyclamH_2, bpy-cyclamNi; n = 2, 4) showing the relative positions of the ground, ^3MLCT, and ^3LF states.

The temperature-dependent lifetimes for $Ru(bpy)_3^{2+}$, $Ru(6\text{-}Mebpy)_3^{2+}$, $Ru(bpy)_2(bpy\text{-}cyclamH_2)^{4+}$, and $Ru(bpy)_2(bpy\text{-}cyclamNi)^{4+}$ were well fit by

$$k_{obs} = 1/\tau = k_0 + k_1 \tag{1}$$

$$k_1 = \frac{A}{\sqrt{kT}} \exp(-E_a/kT) \tag{2}$$

where k_0 is a temperature-independent rate constant and $A = H^2_{AB}\pi^{1/2}/\hbar\lambda^{1/2}$. E_a is an "activation free energy", and the prefactor in eq 2 is the one obtained in the high-temperature limit of the quantum-mechanical expressions derived in multiphonon-radiationless deactivation formalism.[27-29] Equations 1 and 2 are expressions derived from a model that describes the decay of the excited state via two independent channels.[28] The temperature-independent channel, k_0, is ascribed to a transition to the weakly-coupled ground state, while the temperature-dependent channel, k_1, is ascribed to a transition to a strongly-coupled state that decays very rapidly to the ground state.[30] (See Figure 3.) An example of the quality of the fit of the temperature-dependent lifetime data for $Ru(bpy)_2(bpy\text{-}cyclamNi)^{4+}$ to eqs 1 and 2 is shown in Figure 2.

---

(22) Furenlid, L. R.; Renner, M. W.; Szalda, D. J.; Fujita, E. *J. Am. Chem. Soc.* **1991**, *113*, 883.
(23) Ram, M. S.; Bakac, A.; Espenson, H. *Inorg. Chem.* **1986**, *25*, 3267.
(24) Heath, G. A.; Yellowlees, L. J. *J. Chem. Soc., Chem. Commun.* **1981**, 287.
(25) Mabrouk, P. A.; Wrighton, M. S. *Inorg. Chem.* **1986**, *25*, 526.
(26) McClanahan, S. F.; Dallinger, R. F.; Holler, F. J.; Kincaid, J. R. *J. Am. Chem. Soc.* **1985**, *107*, 4853.
(27) Brunschwig, B. S.; Sutin, N. *Comments Inorg. Chem.* **1987**, *6*, 209.
(28) Milder, S. J.; Brunschwig, B. S. *J. Phys. Chem.* **1992**, *96*, 2189.
(29) Jortner, J. *J. Am. Chem. Soc.* **1980**, *102*, 6676.
(30) While most authors assume that the rate of formation of the ^3LF state is rate determining, an alternative is also possible; this is that the ^3MLCT and ^3LF states are in equilibrium and that the rate-determining step is the deactivation of the ^3LF state.[35]

Values of the parameters k_0, A, and E_a obtained from the fits are given in Table IV. For $Ru(bpy)_3^{2+}$ the E_a of 3910 cm^{-1} in CH_3CN determined in this study is consistent with the value reported by Caspar and Meyer;[20] in EtOH the value of E_a determined in this work is 3000 cm^{-1}. For $Ru(bpy)_3^{2+}$ and similar complexes the temperature-dependent decay channel, k_1, of the excited state is ascribed to a strongly-coupled radiationless transition from the ^{3}MLCT state to a ligand-field (^{3}LF) state which rapidly decays to the ground state.[18,20] The values of E_a obtained for the $Ru(bpy)_2L^{n+}$ complexes, with L = 6-Mebpy, bpy-cyclamH_2^{2+}, and bpy-cyclamNi^{2+}, are 2120, 2110, and 2280 cm^{-1} (in CH_3CN) and 2240, 1580 (av) and 1870 (av) cm^{-1} (in EtOH), respectively, with the values for the two pendant complexes in EtOH representing the average of the values obtained for the fast and slow components of the emission decay. The smaller E_a values are the prime reason for the shorter room-temperature lifetimes and lower emission quantum yields for the 6-substituted $Ru(bpy)_2L^{n+}$ complexes. The rate-determining step for the temperature-dependent pathway in the $Ru(bpy)_2L^{2+}$ complexes is assumed to be the rate of formation of the ^{3}LF state.[20,30] In the high-temperature limit of radiationless decay theory $E_a = (\Delta G^\circ + \lambda)^2/4\lambda$, where ΔG° is the free-energy difference and λ is the reorganization parameter between the deactivating ^{3}LF and emissive ^{3}MLCT states. In the case of $Ru(bpy)_2L^{n+}$ complexes, the ^{3}LF state is thought to be higher in energy than the ^{3}MLCT state.[18,20] To the extent that a classical fit of the temperature-dependent data is reasonable, the smaller E_a values imply that in these complexes the free-energy difference, ΔG°, is smaller and/or the reorganization parameter (λ) changes from their values in $Ru(bpy)_3^{2+}$.[28,31] Figure 3 is a schematic energy diagram showing the relative positions of the ground, ^{3}MLCT, and ^{3}LF states.

The reported crystal structure of $Ru(bpy)_2(bpy\text{-}cyclamNi)^{4+}$ affords a reasonable explanation for the changes in E_a. In this complex, the average distance of the Ru–N bonds is 2.072 Å,[9] as compared to 2.056 Å in $Ru(bpy)_3^{2+}$,[32] with the Ru–N bond that includes the nitrogen adjacent to the methylene being 2.143 Å.[33] This longer metal–ligand distance, presumably resulting from steric hindrance between the bpy rings and the methylene bridge, reduces the effective ligand-field strength. This reduction in ligand-field strength is expected to lead to a reduction in the observed E_a through its effect on ΔG° and/or λ.[34]

For $Ru(bpy)_2(bpy\text{-}cyclamH_2)^{2+}$ in EtOH, two independent components are seen in the kinetics of the emission decay, and the relative amplitude of the fast component increases from 40% to 75% as the temperature increases from 165 to 265 K. At 298 K only one component was observed in the decay, and it has a rate constant of 3.8×10^8 s^{-1}, a value on the order of that predicted by extrapolation of eqs 1 and 2 with parameters obtained from the fast component observed at lower temperatures. The slow component is not seen at 298 K, probably because its contribution to the decay is small at this temperature.

Previous work[35] has shown that replacement of one of the bpy ligands of $Ru(bpy)_3^{2+}$ by another ligand or other ligands usually leads to a complex with a shorter room-temperature excited-state lifetime. The decrease in lifetime is usually much less than that observed for the 6-substituted bpy complexes studied here. This shortening of the lifetime is attributed to a number of possible factors including changes in the energy of the MLCT and/or LF states. In many of the complexes deactivation of the ^{3}MLCT state via the ligand-field state becomes unimportant while a new deactivation channel via a thermally-accessible MLCT state becomes dominant at room temperature.[35] For the complexes studied here the shortening of the room-temperature excited-state lifetimes results from an increase in the rate of deactivation via the putative ^{3}LF state. It is also possible that other low-energy excited states, such as a MLCT state, provide channels for deactivation of the lowest ^{3}MLCT state. However, the very good fit of the data to eqs 1 and 2 suggests that the states pictured in Figure 3 are the most significant ones in the radiative and nonradiative decays.

Absorption and emission spectra and excited-state lifetimes and quantum yields have been reported for $Ru(bpy)_n(4,4'\text{-}Me_2bpy)_{3-n}^{2+}$ (n = 0, 1, 2, and 3).[20,25,26] Unlike the complexes studied here, as n increases from 0 to 3, the absorption maximum red-shifts from 443 to 450 nm in acetonitrile, the uncorrected emission maximum also red-shifts from 607 to 642 nm (16.47–15.85 $cm^{-1} \times 10^3$), while the emission lifetime decreases by ~2, from 600 to 335 ns, and the quantum yield decreases by ~3, from 0.042 to 0.014, in H_2O at room temperature.[26] The changes observed in quantum yield and lifetimes for the 4-substituted bpy complexes are much smaller than those observed for the complexes currently under study, thus pointing out the importance of the structural changes produced by substitution at the 6 position of the bpy ligand.

Upon 6-methyl substitution in $Ru(bpy)_3^{2+}$, the absorption maxima of the MLCT bands are slightly blue-shifted in methanol at room temperature, with 454, 448, and 446 nm being observed for $Ru(bpy)_3^{2+}$, $Ru(6\text{-}Mebpy)_3^{2+}$ and $Ru(6,6'\text{-}Me_2bpy)_3^{2+}$, respectively.[36] This shift is similar to the shifts observed for the bpy-cyclam pendant complexes. At 77 K the emission lifetimes (μs) and the quantum yields are 5.3 and 0.376, 4.1 and 0.0968, and 2.5 and 0.0176 for $Ru(bpy)_3^{2+}$, $Ru(6\text{-}Mebpy)_3^{2+}$ and $Ru(6,6'\text{-}Me_2bpy)_3^{2+}$, respectively.[36] The authors suggest[36] that the weaker ligand-field strength in the 6-methyl complexes is a possible cause of the lower quantum yields at low temperature. However, at 77 K the lifetime will be determined by the sum of the radiative and temperature-independent nonradiative decay rates (k_0), neither of which should depend on the energy of the ligand-field state. The small changes in lifetime at low temperature are similar to the changes observed here for k_0 in the 6-substituted complexes.

While the ^{3}MLCT state of $Ru(bpy)_3^{2+}$ is thermodynamically unable to reduce either $Ni(cyclam)^{2+}$ or $Ni(diene)^{2+}$, both nickel complexes quench the emission of $Ru(bpy)_3^{2+}$ with quenching rate constants of 1.5×10^8 and 1.1×10^8 M^{-1} s^{-1}, respectively. The quenching is probably due to collisional energy transfer to a ligand-field state of the nickel. $Ni(tetraene)^{2+}$ quenches the ^{3}MLCT state of $Ru(bpy)_3^{2+}$ with a rate constant that is an order of magnitude faster (2.2×10^9 M^{-1} s^{-1}). The reduction potential

---

(31) Provided that $\Delta G^\circ > 0$, E_a has a minimum at $\lambda = \Delta G^\circ$ with $E_a = \Delta G^\circ$. For all other values of λ, $E_a > \Delta G^\circ$. Thus E_a will increase with increasing ΔG° and will increase with increasing λ if $\lambda > \Delta G^\circ$ but will decrease with increasing λ if $\lambda < \Delta G^\circ$.

(32) Rillema, D. P.; Jones, D. S.; Levy, H. A. *J. Chem. Soc., Chem. Commun.* **1979**, 849.

(33) The ^{3}LF state places electron density into antibonding e_g-type orbitals, which results in expanded Ru–N bonds. These bonds are already somewhat expanded in the ground state of the 6-substituted complexes relative to $Ru(bpy)_3^{2+}$, as evidenced by the structure of $Ru(bpy)_2(bpy\text{-}cyclamNi)^{4+}$. The bond-length changes between the ground and ^{3}LF states are expected to be less for the 6-substituted complexes than for $Ru(bpy)_3^{2+}$.

(34) The reduction in ligand-field strength lowers the vertical or spectroscopic energy, E_{op} between the relevant ligand-field state and the ground state. E_{op} is given by $E_{op} = \Delta G^\circ_{GS,LF} + \lambda_{GS,LF}$, where $\Delta G^\circ_{GS,LF}$ and $\lambda_{GS,LF}$ are the free-energy difference and reorganization parameter between the ground and ^{3}LF states. The absorption and emission spectra indicate that the energy differences and bond-length distortions between the ^{3}MLCT and ground states are similar for the $Ru(bpy)_2L^{n+}$ complexes studied here and $Ru(bpy)_3^{2+}$. Since $\Delta G^\circ_{MLCT,GS}$ and $\lambda_{MLCT,GS}$ (which is a function of changes in bond lengths) between the ^{3}MLCT and the ground states are similar for $Ru(bpy)_3^{2+}$ and the pendant complexes, and $\Delta G^\circ_{LF,GS}$ and/or $\lambda_{LF,GS}$ between the ^{3}LF and ground states change(s), then the ΔG° and/or λ between the ^{3}LF and ^{3}MLCT states will also change. The alternative mechanism, in which the ^{3}MLCT and ^{3}LF states are in equilibrium, still requires that as the position of the ^{3}LF state changes relative to the ground and ^{3}MLCT states, the observed rate of decay of the ^{3}MLCT state also changes.

(35) (a) Barigelletti, F.; Juris, A.; Balzani, V.; Belser, P.; von Zelewsky, A. *J. Phys. Chem.* **1987**, *91*, 1095. (b) Allen, G. H.; White, R. P.; Rillema, D. P.; Meyer, T. J. *J. Am. Chem. Soc.* **1984**, *106*, 2613. (c) Cherry, W. R.; Henderson, L. L., Jr. *Inorg. Chem.* **1984**, *23*, 983. (d) Revco, P.; Schmehl, R. H.; Cherry, W. R.; Fronczek, F. R.; Selbin, J. *Inorg. Chem.* **1985**, *24*, 4078. (e) Juris, A.; Barigelletti, F.; Balzani, V.; Belser, P.; von Zelewsky, A. *Inorg. Chem.* **1985**, *24*, 202. (f) Lumpkin, R. S.; Kober, E. M.; Worl, L. A.; Murtaza, Z.; Meyer, T. J. *J. Phys. Chem.* **1990**, *94*, 239. (g) Barigelletti, F.; Juris, A.; Balzani, V.; Belser, P.; von Zelewsky, A. *Inorg. Chem.* **1983**, *22*, 3335.

(36) Fabian, R. H.; Klassen, D. M.; Sonntag, R. W. *Inorg. Chem.* **1980**, *19*, 1977.

of Ni(tetraene)$^{2+}$ (−0.26 V vs NHE) is in the range where electron-transfer quenching would be expected to occur, and thus the larger quenching rate suggests that most of the quenching by this complex occurs via electron transfer. However, transient absorption measurements failed to reveal the existence of either the Ni^{II}(tetraene)$^+$ radical or $Ru(bpy)_3^{3+}$ after the quenching event, indicating that if electron-transfer quenching does occur, most of the products undergo back electron transfer in the initial solvent cage.

The unimolecular energy-transfer rate constant for the bpy-cyclamNi^{2+} pendant complex can be estimated from the bimolecular quenching data. The rate constant for the bimolecular quenching, k_q, of $Ru(bpy)_3^{2+}$ by Ni(cyclam)$^{2+}$ is 1.5×10^8 M^{-1} s^{-1} at 20 °C. Moreover, $k_q = K_{eq}k_e$, where K_{eq} is the equilibrium constant for the formation of the reactant precursor complex [e.g., $Ru(bpy)_3^{2+}|NiL^{2+}$] and k_e is the first-order rate constant for energy transfer within this complex. The equilibrium constant can be estimated from Debye–Huckel expressions[37] as ~ 0.5 M^{-1}. This gives $k_e \sim 3 \times 10^8$ s^{-1} at room temperature; the rate constant for energy transfer within the pendant complex would be expected to have a similar value. Thus, in the bpy-cyclamNi^{2+} pendant complex the energy-transfer pathway could play an important role in determining the rate of excited-state decay. However, the lifetime of the complex is also expected to be affected by the rate of deactivation of the ^{3}MLCT state via the ^{3}LF state of Ru. This rate constant can be estimated from the lifetime of the bpy-cyclamH_2^{2+} pendant complex and is thus expected to be about 2×10^8 s^{-1} at room temperature, a value similar to the energy-transfer rate constant estimated above. Thus, for the bpy-cyclamNi^{2+} pendant complex near room temperature, deactivation both by a strong-coupling nonradiative decay to a ruthenium-centered ligand-field state and by energy transfer to a nickel-centered ligand-field state may contribute to the rate of deactivation of the ^{3}MLCT state. This suggestion is supported by the difference in k_0 and k_1 for the bpy-cyclamH_2^{2+} and bpy-cyclamNi^{2+} pendant complexes. At all temperatures studied, the observed rates for the slow and fast components of the decay of the bpy-cyclamNi^{2+} pendant complexes in EtOH are faster than the corresponding rates of the bpy-cyclamH_2^{2+} pendant complex. This is also true for the calculated value of k_1 at room temperature. Likewise, k_0 is larger for the nickel complex, while the energy gap ($\Delta G°$) between the emissive ^{3}MLCT state and the ground state for the two complexes is similar. Thus the energy-transfer pathway may contribute to the low-temperature rate.[38]

Conclusions

1. For $Ru(bpy)_2bpy{-}L^{2+}$ complexes substituted at the 6 position of the bipyridine ring, steric hindrance by the 6-methyl group or the 6-methylene bridge causes an increase in the Ru–N bond distance, a decrease of the ligand-field strength, and a lowering of the energy of the excited ligand-field states and/or changes in their metal–ligand distortion (λ) relative to the ^{3}MLCT and ground states. These changes dramatically decrease the lifetimes of the ^{3}MLCT excited state of these complexes near room temperature due to an increase in the temperature-dependent deactivation rate via a strongly-coupled ligand-field state.

2. For the $Ru(bpy)_2$(bpy-cyclamNi)$^{4+}$ complex, two channels may contribute to the excited-state decay at room temperature. Deactivation takes place via strong coupling to a ruthenium-centered ligand-field excited state and possibly via energy transfer to a nickel-centered ligand-field state. Thus the observed quenching of the ^{3}MLCT state is due entirely to enhancement of the nonradiative decay channels.

3. The enhancement of the ligand-field decay channels in these 6-substituted Ru(bpy) complexes is an undesirable complication in catalytic systems. When a mediator or catalyst is attached to a photosensitizer, the substitution should not either lower the energy of any of the sensitizers's deactivating excited states or introduce low-energy excited states on the mediator which quench the sensitizer. Either case will reduce the yield of the desired electron-transfer quenching pathway and decrease catalytic activity.

Acknowledgment. We thank Drs. Carol Creutz and Norman Sutin for helpful discussions, Dr. Siegfried Schindler for synthetic suggestions, and Elinor Norton for analyses for ruthenium, nickel, PF_6^-, and ClO_4^- and measurements of mass spectra. This research was carried out at Brookhaven National Laboratory under Contract DE-AC02-76CH00016 with the U.S. Department of Energy and supported by its Division of Chemical Sciences, Office of Basic Energy Sciences.

---

(37) Sutin, N.; Brunschwig, B. S. *ACS Symp. Ser.* **1982**, *No. 198*, 105.

(38) It would be expected that this pathway would have a temperature-dependent rate. However, extraction of another set of activation parameters from the data is not possible.

Contribution from the Arthur Amos Noyes Laboratory,[†] California Institute of Technology,
Pasadena, California 91125, and Department of Chemistry, University of Pittsburgh, Pittsburgh, Pennsylvania 15260

Fluorescence Excitation Spectra of Quadruply Bonded $M_2X_4L_4$ Complexes

Vincent M. Miskowski,*[‡] Harry B. Gray,*[‡] and Michael D. Hopkins*[§]

Received August 19, 1991

Fluorescence excitation spectra have been obtained by monitoring the emissive $^1(\delta\delta^*)$ excited states of $Mo_2X_4(PMe_3)_4$ (X = Cl, Br, I), $Mo_2Cl_4(AsMe_3)_4$, and $W_2Cl_4(PMe_3)_4$ in solution at 300 and 77 K. The polarization ratios of these transitions, and their shifts in energy arising from substitution of the metal and ligand, have been correlated with predictions derived from available theoretical calculations and photoelectron spectroscopic data to yield self-consistent assignments of all observed bands in the UV region. These bands, with the exception of a poorly characterized one at the edge of the vacuum-UV region, are assigned to singlet excitations from metal–metal (δ, σ, π) and ligand (σ(MP), σ(MX), π(X)) orbitals to the δ^* orbital.

Complexes of the $M_2X_4L_4$ class (M = Mo, W; X = Cl, Br, I; L = P or As donor) have proven to be valuable subjects of research into the nature and properties of the metal–metal quadruple bond, in large part because the wide range of systematic electronic perturbations that can be achieved through ligand and metal substitution allows elucidation of metal–metal and metal–ligand properties.[1,2] Although most of the attention devoted to these compounds has focused on the δ and δ^* orbitals and the electronic

---

[†] Contribution No. 8499.

[‡] California Institute of Technology.

[§] University of Pittsburgh.

(1) (a) Hopkins, M. D.; Miskowski, V. M.; Gray, H. B. *J. Am. Chem. Soc.* **1988**, *110*, 1787–1793. (b) Hopkins, M. D.; Schaefer, W. P.; Bronikowski, M. J.; Woodruff, W. H.; Miskowski, V. M.; Dallinger, R. F.; Gray, H. B. *J. Am. Chem. Soc.* **1987**, *109*, 408–416. (c) Hopkins, M. D.; Zietlow, T. C.; Miskowski, V. M.; Gray, H. B. *J. Am. Chem. Soc.* **1985**, *107*, 510–512. (d) Zietlow, T. C.; Hopkins, M. D.; Gray, H. B. *J. Solid State Chem.* **1985**, *57*, 112–119. (e) Hopkins, M. D.; Gray, H. B. *J. Am. Chem. Soc.* **1984**, *106*, 2468–2469. (f) Hopkins, M. D. Ph.D. Thesis, California Institute of Technology, 1986.

0020-1669/92/1331-2085$03.00/0